Fault Interaction in Alaska: Static Coulomb Stress Transfer

Charles G. Bufe

U.S. Geological Survey, Golden, Colorado, USA

Oliver S. Boyd

U.S. Geological Survey, Memphis, Tennessee, USA

Between 1938 and 2002, most of the known major active fault segments in southern Alaska with estimated recurrence intervals of less than 700 years have ruptured. Static (coseismic) Coulomb stress transfer has been modeled from the nine largest ($M \geq 7.5$) of these earthquakes. Stresses transferred from these sources, ranging from less than 0.001 MPa (0.01 bar) to 1 MPa (10 bars) locally, were computed on 30 target fault segments, including 16 segments associated with the above major earthquake sources. Post-1938 cumulative static Coulomb stress transfer in excess of 0.1 MPa preceded failure of the Denali–Totschunda, Sitka, Kodiak, and southern Gulf of Alaska segments. Stress transfer since 1938 indicates the presence of transferred stresses in excess of 0.1 MPa, locally approaching 1 MPa, at seismogenic depths on target fault segments that have not ruptured since 1938, including the Denali Park segments of the western Denali fault, the Castle Mountain fault, the Cross Creek fault, the southern part of the Totschunda–Fairweather gap, and the west Yakataga gap. Some segments that have ruptured during or since 1938 have received static Coulomb stress reloading locally in excess of 0.1 MPa. These include the Alaska Peninsula, offshore Fairweather, and northern Queen Charlotte fault segments. Stresses transferred to the slowly slipping Denali–Totschunda fault system can result in significant earthquake probability changes, whereas high slip rates on the Fairweather–Queen Charlotte transform fault system limit the advance toward (or retreat from) time of failure due to transferred stresses.

1. INTRODUCTION

After the great 1938 *M* 8.2 Semidi earthquake on the Alaska Peninsula segment of the Alaskan–Aleutian megathrust (see Plate 1), seismic moment release rate along the northeastern edge of the Pacific plate increased dramatically, with major fault segments rupturing from British Columbia (130°W, longitude) out to 170°E (longitude), near the western end of the Aleutian chain. The largest of these earthquakes were the *M* 9.2 Prince William Sound earthquake of March 28, 1964, and the *M* 8.7 Rat Islands earthquake of February 4, 1965. Other great events included the *M* 8.1 Queen Charlotte Islands transform earthquake of August 22, 1949, the *M* 8.1 tsunami earthquake south of Unimak Island on April 1, 1946, and the *M* 8.6 Central Aleutians earthquake of March 9, 1957. The latter two events occurred along the Aleutian megathrust. The moment magnitude of the great 1957 earthquake has been downgraded from 9.1 to 8.6 as a result of studies by *Johnson et al*. [1994]. Two segments

Active Tectonics and Seismic Potential of Alaska
Geophysical Monograph Series 179
This paper is not subject to U.S. copyright. Published in 2008 by the American Geophysical Union.
10.1029/179GM24

that ruptured in the 1957 event have reruptured since: the Andreanof Islands segment in 1986 (M 8.0) and the Delarof Islands segment in 1996 (M 7.9). The latter event was forecast by *Bufe et al*. [1994] based on the time-to-failure analysis of accelerating seismic release [*Bufe and Varnes*, 1993]. This approach was also used by *Bufe* [2004a] in hindsight to document accelerating seismic release preceding the 2002 Denali fault earthquake. Between 1938 and 1965, nearly all of the northeastern Pacific plate boundary appears to have ruptured [*Nishenko and Jacob*, 1990].

In this chapter, we examine coseismic Coulomb stress transferred since 1938 by large ($M \geq 7.5$) earthquakes in southern Alaska, east of 160°W longitude. Our objectives are to determine whether static Coulomb stress transfer contributed to the occurrence of the larger earthquakes since 1938 and to identify fault segments that may have been moved significantly closer to failure in future large earthquakes.

2. STRESS MODELING

The program used to compute displacements and in-plane stresses is 3d-def, a three-dimensional boundary element program developed by *Gomberg and Ellis* [1994] that uses

Table 1. Alaska $M \geq 7.5$ Source Models[a]

Year	X, km	Y, km	Z, km	L, km	W, km	Strike, cm	Dip	Strike-Slip	Thrust
Alaska Peninsula, Semidi [after Johnson and Satake, 1994]									
1938	−658	−450	−5	300	150	245	10	−0	210
Queen Charlotte [Pacheco and Sykes, 1992; Plafker et al., 1994; Bufe, 2005]									
1949	725	−680	−0	321	12	324.2	90	−800	0
	825	−768	−0	133	12	311.3	90	−800	0
Fairweather [Pacheco and Sykes, 1992; Plafker et al., 1994; Bufe, 2005]									
1958	400	−156	−0	227	12	320	90	−440	0
	451	−256	−0	110	12	333	90	−440	0
PWS-Kodiak source model of Johnson et al. [1996]									
1964	−425.83	−375.86	−3	100	100	218	8	0	0
	−370.20	−320.90	−3	100	100	218	8	0	550
	−302.14	−248.36	−3	100	100	218	8	0	1450
	−235.20	−173.61	−3	100	100	218	8	0	70
	−151.91	−155.46	−2	90	100	230	8	844	1646
	−82.86	−116.28	−1	90	100	242	8	279	1014
	−6.81	−92.63	−1	90	100	256	8	18	410
	−512.51	−304.04	−17	100	100	218	9	0	410
	−435.64	−252.63	−17	100	100	218	9	0	0
	−367.23	−181.20	−17	100	100	218	9	0	460
	−301.62	−107.42	−17	100	100	218	3	349	720
	−204.54	−70.32	−16	120	100	229	3	604	2126
	−118.78	−23.77	−15	120	100	241	3	113	1786
	−22.13	3.42	−15	120	100	256	3	233	520
	−269.37	49.05	−21	130	100	219	3	20	67
	−148.55	66.68	−20	130	100	241	3	162	2083
	−35.00	102.86	−20	130	100	256	3	61	788
	−184.08	10.20	−0.1	72	30	219	60	0	850
Fairweather, Sitka [Schell and Ruff, 1989; Page et al., 1991; Bufe, 2005]									
1972	544	−433	−0	190	12	333	90	−440	0
St. Elias, Coal Glacier [Stephens et al., 1980; Plafker et al., 1994; Global CMT Catalog, 2007]									
1979	222	1	−2	90	90	271	13	0	80
Gulf of Alaska, N [Choy and McGarr, 2002]									
1987	70.8	−83	−3	112	20	180	90	−1070	0
Gulf of Alaska, S [Choy and McGarr, 2002]									
1988	73	−202	−4	125	20	180	90	−650	0
Denali fault [Eberhart-Phillips et al., 2003; Frankel, 2004; Hreinsdottir et al., 2003, 2006]									
2002	75	259	−0	72	12	323	90	−225	0
	30	321	−0	145	18	296	90	−744	0
	−102	386	−0	55	18	279	90	−585	0
	−148	386	−0	36	18	270	48	−150	330

[a] Origin of coordinates: 60.00°N, 144.00°W. Cartesian grid overlain on Albers equal area projection for standard parallels 55° and 65°. Most coordinates and fault lengths are scaled from the map of *Plafker et al*. [1994].

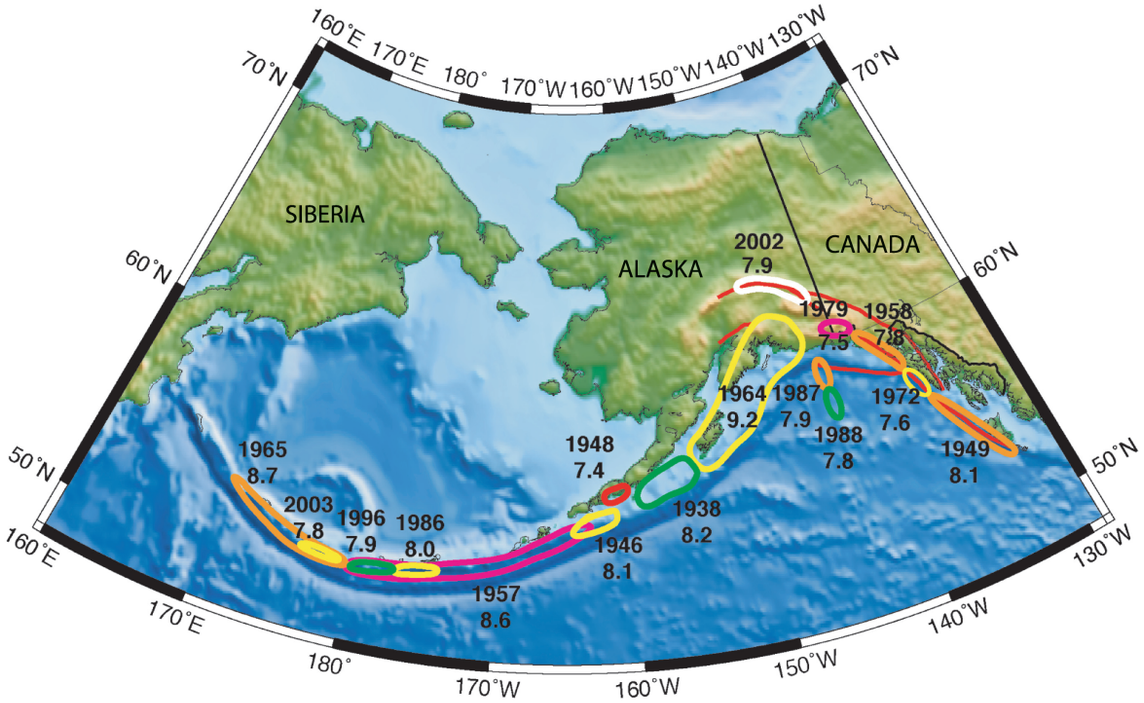

Plate 1. Dates of principal earthquakes in Alaska with their rupture/aftershock zones (modified from *Wesson et al*. [1999]).

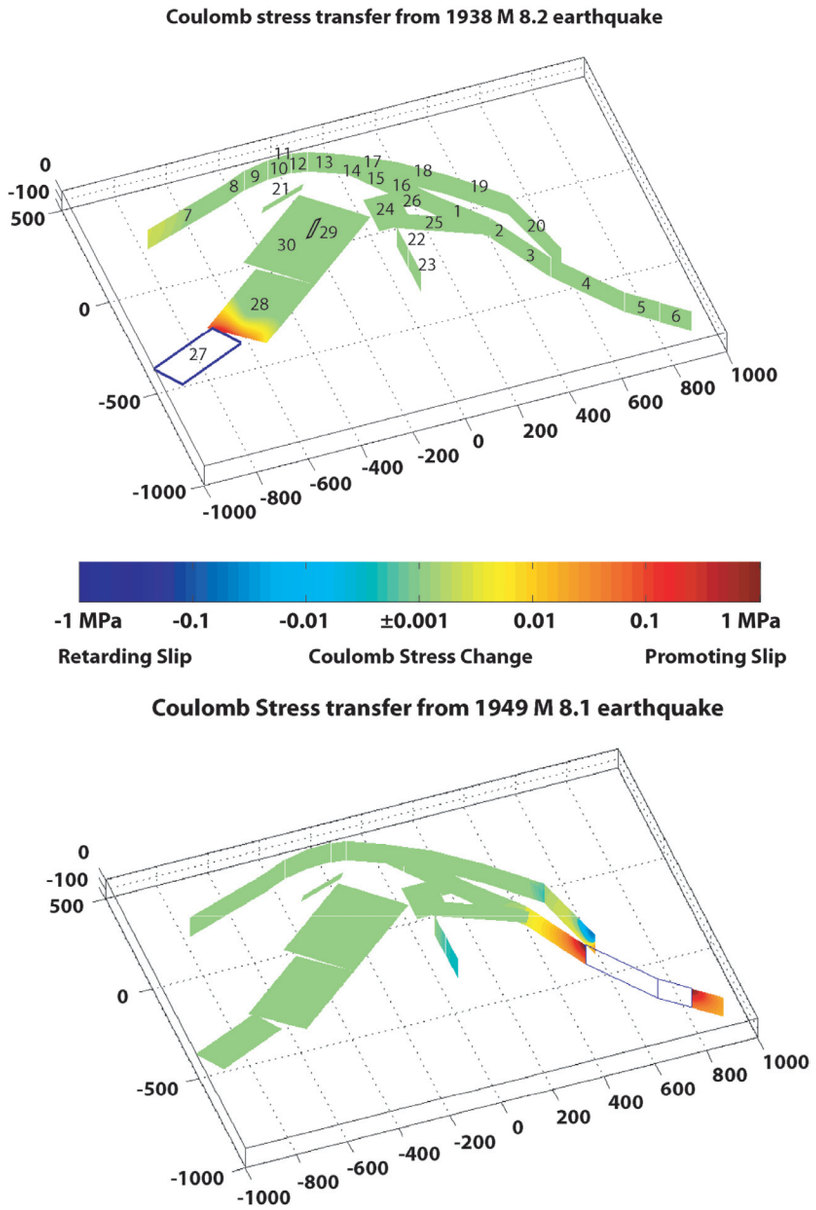

Plate 2. (a, above the color bar) View looking N20°E and showing static Coulomb stress transferred in the rupture of the *M* 8.2 Semidi (Alaska Peninsula) earthquake of 1938. The fault plane of the source event is outlined in black. The 30 target segments used in this study are numbered here in the sequence listed in Table 2. (b, below the color bar) The *M* 8.1 Queen Charlotte earthquake of 1949. The downward-extended fault planes of the shallow strike-slip source are outlined in black.

Green's functions calculated with the routines of *Okada* [1992]. Green's functions describe the deformation field from a rectangular dislocation in a homogeneous elastic half-space. A Poisson's ratio of 0.25 and a Young's modulus (E) of 7×10^{10} Pa are assumed in this study.

3. COULOMB STRESS CHANGE

Coulomb failure stress changes were computed from the modeled shear and normal stress transferred to a given fault plane using the relation:

$$\delta\sigma_c = \delta\tau_s - \kappa(\delta\sigma_n - \delta p) = \delta\tau_s - \kappa'\delta\sigma_n, \quad (1)$$

where $\delta\sigma_c$ is the Coulomb stress change, $\delta\tau_s$ is the change in shear stress on the fault plane in the slip direction, $\delta\sigma_n$ is the change in fault-normal compression, δp is change in pore pressure, and κ is the coefficient of friction. The coefficient of effective friction, κ', is taken here as 0.4. This value, which is consistent with pore pressures of about one-third the fault-normal compression, lies at the center of the range 0.2–0.6, and is often used in Coulomb stress modeling, as in *Toda et al*. [2005]. *Bird* [1996] has inferred a somewhat weaker κ' (0.17) for Alaska faults from neotectonic modeling using a finite-element grid. The pore pressure change can be related to the change in mean stress or confining pressure using the relation:

$$\delta p = B(\delta\sigma_{xx} + \delta\sigma_{yy} + \delta\sigma_{zz})/3, \quad (2)$$

where B is the Skempton coefficient and the expression in parentheses is the mean compressive stress. If the value of B were known, the pore pressure change could be calculated

Table 2. Alaska Target Faults[a]

No.	Year	Segment	X	Y	Z	Strike	Dip	L, km	W, km
1	1958	Fairweather_N	400	−156	−0.1	320	90	227	100
2	1958	Fairweather_S	451	−256	−0.1	333	90	110	100
3	1972	Fairweather_Sitka	544	−433	−0.1	333	90	190	100
4	1949	Q_Charlotte_Nrup	725	−680	−0.1	324.2	90	321	100
5	1949	Q_Charlotte_Srup	825	−768	−0.1	311.3	90	133	100
6		Cape_St_James	918	−854	−0.1	311.3	90	123	100
7		DenaliSW1	−424	336	−0.1	250	90	375	100
8		Denali_Park_West	−348	373	−0.1	245	90	90	100
9		Denali_Park_East	−250	394	−0.1	257	90	99	100
10		Denali_Nenana–Susitna	−160	398	−0.1	267	90	90	100
11	2002	Susitna_Glacier	−148	386	−0.0	270	48	36	18
12	2002	Denali_rup_W	−102	386	−0.0	279	90	55	100
13	2002	Denali_rup_E	30	321	−0.0	296	90	145	100
14	2002	Totschunda_rup	75	259	−0.0	323	90	72	100
15		Cross_Creek	145	160	−0.1	323	90	123	100
16		Totsch_Fair_gap	256	16	−0.1	324	90	183	100
17		Denali_E1	176	232	−0.1	301	90	170	100
18		Denali_E2	324	108	−0.1	310	90	194	100
19		Denali_E3	504	−71	−0.1	315	90	253	100
20		Chatham_Strait	589	−388	−0.1	345	90	330	100
21		Castle_Mtn	−170	238	−0.1	250	75	189	30
22	1987	Gulf_AKN	71	−83	−3.0	180	90	112	100
23	1988	Gulf_AKS	73	−202	−4.0	180	90	125	100
24		Yakataga_gap_W	130	−80	−5.0	270	0	125	170
25		Transition	377	−236	−4.0	298	13	400	100
26	1979	Coal_Glacier	222	1	−2.0	271	13	90	90
27	1938	Semidi	−658	−450	−5.0	245	10	300	150
28	1964	Kodiak	−306	−257	−5.0	230	10	350	250
29	1964	Patton	−184	10	−0.1	219	60	72	30
30	1964	PWS	0	0	−5.0	230	7	400	300

[a] Origin of coordinates: 60.00°N, 144.00°W. Cartesian grid overlain on Albers equal area projection for standard parallels 55° and 65°. Most coordinates and fault lengths are scaled from the map of *Plafker et al*. [1994].

from the change in mean stress. This would allow calculation of the coefficient of friction. However, B can vary from 0 to 1 and depends on the rock type and hydrologic regime at seismogenic depths. Unless this information and its variability are known, the determination of κ' remains highly uncertain. For end-on stress transfer between aligned fault segments, $\delta\tau_s$ dominates equation (1) and the uncertainty of κ' is not a problem. For situations where $\delta\sigma_n$ dominates, such as the transfer from the great 1964 Prince William Sound earthquake to the Denali fault, uncertainty in κ' could easily translate to uncertainty in the Coulomb stress change of a factor of 2. In this chapter, a positive stress change is one that moves the fault closer to failure. Thus, for stress transferred to a right-lateral strike-slip fault, positive $\delta\tau_s$ would be right-lateral and negative $\delta\tau_s$ would be left-lateral stress change.

4. SOURCES AND TARGETS

The parameters of each source ($M \geq 7.5$) are detailed in Table 1. The target faults are listed in Table 2, with each segment designated by a number, keyed to Plate 2a. For target segments that are also source segments during the 1938–2002 interval, the source and target geometries are the same, with one exception. For the great earthquake of 1964, a detailed source model (16 segments) was derived by *Johnson et al*. [1996] from a joint inversion of tsunami and geodetic data. The corresponding target faults for transfer from other ruptures are the simplified Prince William Sound and Kodiak segments used by *Bufe* [2004b] in modeling stress transfer from the great 1964 earthquake.

Coulomb stresses are computed and shown in the plates down to 100 km depth. This depth was deliberately chosen because the static stresses are effectively transferred well below the locking depth. As relaxation occurs through creep or viscoelastic flow, these transferred stresses will contribute to postearthquake deformation, both below the source and target faults, reloading the shallower locked zones.

The Coulomb stresses transferred from the largest sources in Table 1 to each target in Table 2 are shown in Plates 2–5. In each plate, the source segments are outlined. For the vertical strike slip faults, the entire target segment down to 100 km is outlined for simplicity although rupture is modeled only on the uppermost 12 km for the Totschunda segment of the 2002 Denali earthquake and for the Queen Charlotte and Fairweather fault earthquakes [see also *Bufe*, 2005] based on an average of the locking depth estimates given by *Fletcher and Freymueller* [2003] and by *Mazzotti et al*. [2003]. For the 2002 Denali fault segments, rupture was modeled down to 18 km, as indicated by the GPS-derived coseismic slip distribution of *Hreinsdottir et al*. [2003].

A logarithmic color bar developed by *Bufe* [2004b] is used for these plates. Zero on this colorbar scale corresponds to the log to the base 10 of an absolute stress value of 0.001 MPa. All stresses smaller than ±0.001 MPa are set to this value. Positive values represent Coulomb stress changes that move the fault closer to failure, negative away from failure.

5. RESULTS

Examination of change in Coulomb failure stress (Plates 2–5) shows varying degrees of advance toward or retreat from failure as a result of earthquake stress transfer. For most sources, the target segments are predominantly moved toward failure by Coulomb stress transfer.

The initial event in the sequence, the M 8.2 Semidi earthquake of November 10, 1938, occurred opposite a major confining bend in the strike of the Aleutian trench along the Alaska Peninsula (map of *Plafker et al.* [1994]). For gravity-driven slip components perpendicular to the trench, this results in convergence and compression parallel to the trench, making this segment a keystone for the Aleutian megathrust. This change in strike is aligned with a prominent lineament seen in Plate 1. This lineament, which trends about N13°W, can be traced intermittently over a distance of 900 km from Dillingham (59.0°N, 158.5°W) to the vicinity of Kotzebue (66.9°N, 162.6°W) in Alaska. It disrupts topographic features and fault patterns and in its central portion coincides with the left-lateral Thompson Creek fault. It is, however, absent on some high-resolution topographic maps, and may be an artifact.

The source model of the 1938 earthquake is based on the single segment version of the model of *Johnson and Satake* [1994]. Stresses of 0.1 MPa were transferred to the southwestern end of the Kodiak segment (Plate 2a). All fault segments are numbered in Plate 2a, coded to target segments whose coordinates and dimensions are described in Table 2.

The next event in the sequence was the M 8.1 Queen Charlotte earthquake of August 22, 1949. This earthquake ruptured about 450 km of the transform system, from about 100 km south of Sitka, Alaska, to 100 km northwest of Cape St. James, British Columbia, Canada. Stresses up to 1 MPa were transferred to the Sitka segment of the Fairweather fault to the northwest and the Cape St. James segment of the Queen Charlotte fault to the southeast (Plate 2b). Tectonic loading and Coulomb stress transfer along the Fairweather–Queen Charlotte transform system are discussed in detail by *Bufe* [2005].

On July 10, 1958, an M 7.8 earthquake ruptured the two northernmost segments of the Fairweather fault, triggering a landslide into Lituya Bay that generated a large local tsunami. Coulomb stresses from this rupture loaded the north-

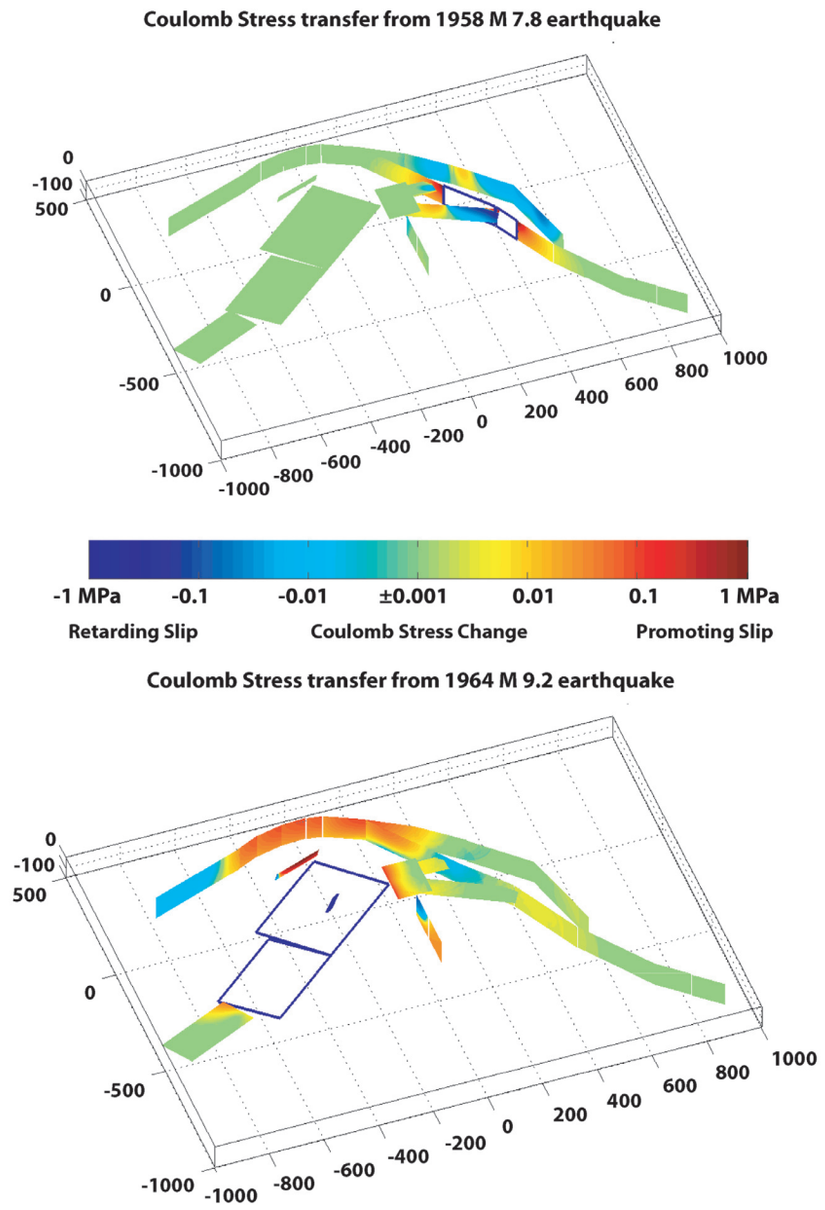

Plate 3. View looking N20°E and showing static Coulomb stress transferred in the rupture of: (a, above the color bar) the *M* 7.8 Fairweather (Lituya Bay) earthquake of 1958. The downward-extended fault planes of the shallow strike-slip source are outlined in black. (b, below the color bar) The great *M* 9.2 Prince William Sound earthquake of 1964. The 18 segments used in the source model are represented in the plate by simplified Prince William Sound, Kodiak, and Patton Bay fault planes outlined in black.

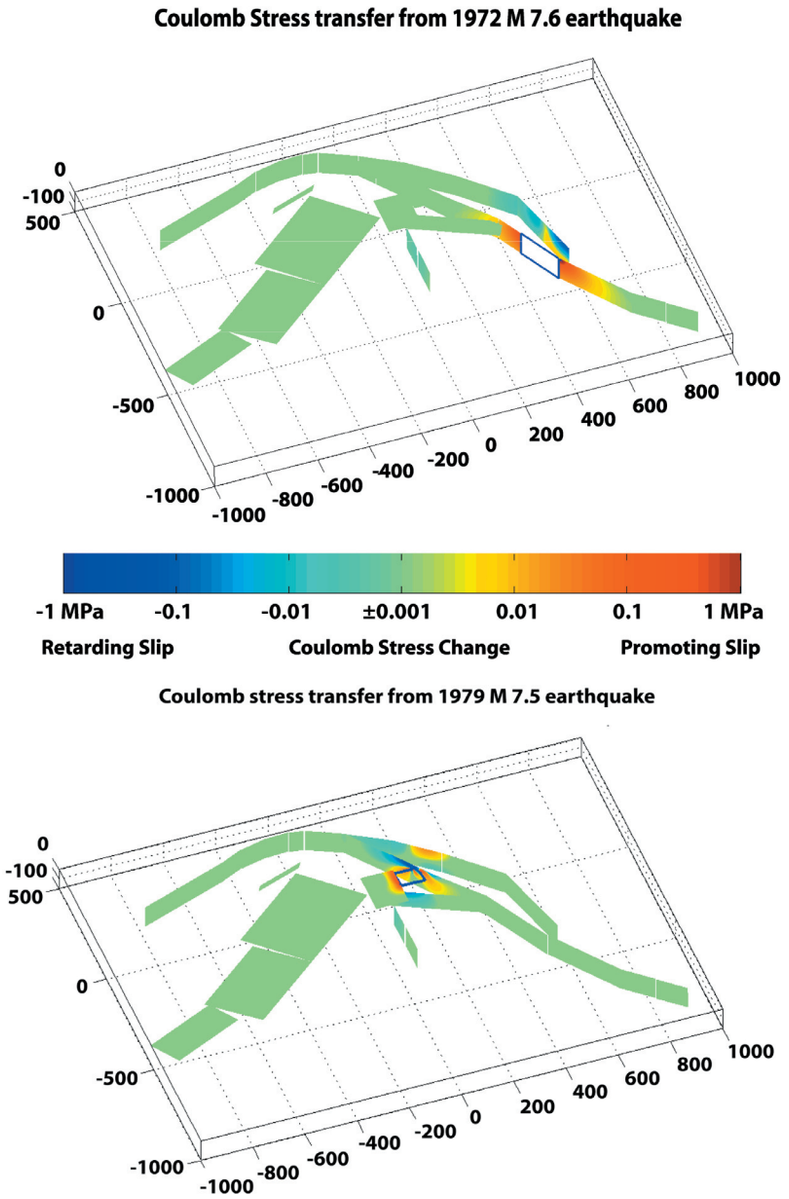

Plate 4. View looking N20°E and showing static Coulomb stress transferred in the rupture of: (a, above the color bar) the *M* 7.6 Sitka earthquake of 1972. The downward-extended fault plane of the shallow strike-slip source is outlined in black. (b, below the color bar) The *M* 7.5 Coal Glacier earthquake of 1979. The fault plane of the source earthquake is outlined in black.

western part of the Sitka segment of the Fairweather fault by up to 1 MPa locally (Plate 3a). This transfer, combined with the stresses transferred from the 1949 Queen Charlotte earthquake and the great 1964 earthquake, may have set the stage for the 1972 Sitka event, which occurred in an obvious seismic gap [*Schell and Ruff*, 1989]. The 1972 rupture (Plate 4a) appeared to be bilateral, with the hypocenter near the junction of the two fault segments and away from the areas of high positive Coulomb stress transfer.

At *M* 9.2, the 1964 Prince William Sound earthquake is by far the dominant earthquake in the region. *Bufe* [2004b] modeled Coulomb stress transfer from this earthquake to the Denali fault and other prominent faults in the region, using a simple two-segment (Prince William Sound and Kodiak) source model. In the present chapter, we use the more detailed (18-segment) 1964 earthquake source model of *Johnson et al*. [1996], although the outline of the simple two-plane model is shown in the plate (Plate 3b). The results for the two models are very similar, except for details of stress transfer within a few tens of kilometers, such as on the northern Gulf of Alaska segment. A significant positive Coulomb stress of 0.1 MPa was transferred to large areas of the northern Denali and Totschunda faults, primarily by reduction of normal stress (Plate 3b).

The earthquake of July 30, 1972, on the Sitka segment of the Fairweather fault transferred positive Coulomb stress of up to 1 MPa (Plate 4a), primarily to the adjacent segments of the Fairweather and Queen Charlotte faults.

The St. Elias earthquake of February 28, 1979, ruptured an approximately 90 × 90 km (from aftershocks) north-dipping segment of the Coal Glacier thrust fault [*Stephens et al*., 1980; *Global CMT Catalog*, 2007]. Stress transfer from this relatively small event (Plate 4b) was very local, but significant (0.1 MPa) positive Coulomb stresses were transferred to the adjacent parts of the Yakataga gap and comparable negative Coulomb stresses to seismogenic depths of the Totschunda–Fairweather gap. *Estabrook et al*. [1992] have determined a more complex, multiple-source model for this earthquake, with a more northeasterly slip direction. The nearest segment of the 1979 rupture is more than 150 km away from the 2002 Denali–Totschunda rupture, so the model differences would not significantly affect the stresses transferred there.

On November 30, 1987, and on March 6, 1988, two large north-striking right-lateral earthquakes occurred in the northern Gulf of Alaska. *Choy and McGarr* [2002] have estimated that these high-stress earthquakes within the Pacific plate ruptured to depths of at least 20 km. *Sauber et al*. [1993] calculated the static displacements associated with the 1987–1988 Gulf of Alaska earthquakes and compared them to geodetic data. They also estimated the possible influence of the 1964 earthquake on these events. The initial, northernmost event had the same moment magnitude (7.9) as the 2002 Denali fault earthquake, but with only about a third the fault length. With this moment and geometry, the mean slip used in modeling stress transfer exceeds 10 m. This event had exceptionally high apparent stress, possibly the highest in the USGS energy magnitude catalog (George Choy, personal communication 2005). Coulomb stress transferred by this November 30, 1987 event is shown in Plate 5a. The segment to the south that ruptured on March 6, 1988, was moved uniformly toward failure by Coulomb stress changes exceeding 0.1 MPa, with local values approaching 1 MPa. Coulomb stress augmentations and shadows of ±0.01 MPa were cast out to distances of 500 km. By contrast, stress transferred (not shown) from the *M* 7.8 southern Gulf of Alaska event of March 6, 1988, raised the Coulomb stress on the shallow, seismogenic region of the northern Gulf of Alaska segment by up to 0.1 MPa, but had little effect on other target segments.

The 2002 Denali earthquake source model is based on the rupture modeling of *Frankel* [2004], with depth information from *Hreinsdottir et al*. [2003]. The Denali fault earthquake of November 3, 2002, transferred stresses in excess of 0.1 MPa (locally 1 MPa) to the adjacent Denali fault segment to the west (Nenana–Susitna segment) and to the Cross Creek segment of the Totschunda fault to the southeast (Plate 5b). The adjacent eastern segment (Denali E1) is loaded in excess of 0.1 MPa (locally 1 MPa) for about 110 km and then falls in a 0.1-MPa stress shadow at seismogenic depths for 100 km to the east. The northern edge of the great Prince William Sound asperity is loaded to about 0.005 MPa. *Anderson and Ji* [2003] have also modeled stress transfer from the Denali earthquake and from its Nenana Mountain foreshock. They demonstrated that stress transferred from the *M* 6.7 foreshock may have triggered the event on the Susitna Glacier thrust fault that initiated the predominately strike slip *M* 7.9 Denali fault earthquake.

6. CUMULATIVE COSEISMIC COULOMB STRESS CHANGES BEFORE SEGMENT FAILURE

The cumulative sum of coseismic Coulomb stress transferred to each source segment, before the post-1938 rupture of that segment, is shown in Plate 6a. The source segments of the nine $M \geq 7.5$ earthquakes are outlined for easy recognition. For other target segments that did not rupture during 1938–2005, the total coseismic Coulomb stress transferred is shown. Stresses in excess of 0.1 MPa were transferred to several of the source segments during the 1938–2002 period. These include the Kodiak, Denali, Totschunda, Sitka, and southern Gulf of Alaska segments. The fault segments are

numbered in Plate 2a, coded to segments described in Table 2. Posttransfer remaining times to failure for these segments ranged from 3 months to 38 years, indicating that the segments were nearing the end of their recurrence cycles and/or were triggered by large, time-dependent postearthquake stress transfer processes discussed by *Boyd et al*. [this volume]. Coulomb stress transfer was likely a strong contributing factor to the triggering of the *M* 7.8 1988 Gulf of Alaska and the *M* 7.9 2002 Denali fault earthquakes, and to a lesser degree the *M* 7.6 Sitka earthquake of 1972 [*Bufe*, 2005]. In the case of the Kodiak segment, stress transferred from the 1938 Semidi event did not contribute to the initiation of the great 1964 Prince William Sound earthquake, but may have extended its rupture length. Ruptures that occurred early in the sequence, such as the 1949 Queen Charlotte event, had little opportunity to accumulate significant prerupture Coulomb stress transfer.

7. POSTRUPTURE STATIC STRESS TRANSFER: IMPLICATIONS FOR SEISMIC HAZARD

The cumulative sum of static Coulomb stress transfer to each target segment, since 1938 or since the post-1938 rupture of that source segment, is shown in Plate 6b. The target segments that have received substantial positive cumulative static Coulomb stress transfer (0.1 MPa or greater) are the Castle Mountain fault, the Denali Nenana–Susitna and Denali Park east and west segments, the Cross Creek segment of the Totschunda fault, the southern end of the Totschunda–Fairweather gap, the northern and southern ends of the Fairweather fault, the northern and southern (Cape St. James) ends of the Queen Charlotte fault, and parts of the Yakataga gap. In contrast, the eastern end of the Transition fault, the southern end of the Chatham Strait fault, the northwestern end of the Totschunda–Fairweather gap, and the southeastern part of the first Denali east segment are moved away from failure by at least 0.1 MPa at seismogenic depths.

In June 2004, a magnitude 6.8 earthquake occurred along the northern Queen Charlotte fault, the largest on this segment since the *M* 8.1 earthquake of 1949. This is consistent with the relatively high transferred stress and the reloading (up to 0.06 MPa/a) since 1949 [*Bufe*, 2005]. The northern part of the southernmost Queen Charlotte fault (Cape St. James segment) is believed by *Rogers* [1986] to be a possible rupture gap between the 1949 earthquake and a smaller *M* 7.3 event that occurred at the southern end of this segment in 1970.

The cumulative postrupture transferred static Coulomb stress map bears primarily on the spatial distribution of earthquake hazard, but must be combined with information on tectonic loading rates to be meaningful [*Hardebeck*, 2004; *Parsons*, 2005; *Bufe*, 2005]. The criterion of *Parsons* [2005] that the ratio of Coulomb stress change to tectonic stressing rate should be on the order of 10:1 to 20:1 is not met in many cases, especially along the edges of the rapidly moving Pacific plate. On the slow-moving Denali, Cross Creek, and Castle mountain segments, these criteria may be met. Where rapid slip occurs along the transform and the megathrust, cumulative loading dominates, and the clock advance or shortening of recurrence interval due to the Coulomb stress transfer is negligible. The 1938 Semidi segment may be nearing rupture, based on tectonic loading [*Bufe*, 2006].

The best approach for using Coulomb stress transfer in assessing time-varying earthquake hazard is still in the research stage. As demonstrated by *Parsons* [2005], the uncertainties are large. The time interval between the transfer of stress from the earthquake source and the occurrence of an earthquake on the target fault is highly variable. From the clustering statistics described earlier, elastic Coulomb stress transfer, which occurs almost instantaneously in time and is relatively localized in space, does not appear to be the direct mechanism for triggering of most large earthquakes in Alaska. Even in cases here where strong positive Coulomb stress transfer is followed by the occurrence of a large earthquake on a target fault, there is a ubiquitous time lag. An example is the 97 days between the 1987 and 1988 Gulf of Alaska earthquakes discussed above. Another is the 92 days between the great Sumatra earthquakes of December 26, 2004, and March 28, 2005. What process loads the fault the final increment to failure? Given the long recurrence intervals, interim tectonic loading does not appear as the likely answer.

One can easily envision a tectonic regime in which fault systems evolve to accommodate a self-consistent pattern of regional deformation, where failure of each segment eventually leads to failure of others. The Alaska syntaxis may be such a regime. Under these conditions, each rupture would tend to be in an optimal position relative to other, previous ruptures. Coulomb stress transfer would be almost universally positive. Coulomb stress transfer, although favorable to triggering, is probably not the controlling factor. There is some other intrinsically time-dependent process that ultimately triggers most earthquakes. Perhaps it is rate and state friction [*Dieterich*, 1994; *Parsons et al*., 2000]. Perhaps this process is not initiated by coseismic Coulomb stress transfer. There may be some physical property that is changed by dynamic strain during the passage of seismic waves, strain that rapidly becomes orders-of-magnitude larger than the static strain as we move away from the source [*Gomberg, et al*., 2004]. Perhaps aseismic rupture is triggered near the base of the seismogenic zone or on poorly coupled fault patches, concentrating stress around major asperities. The downward

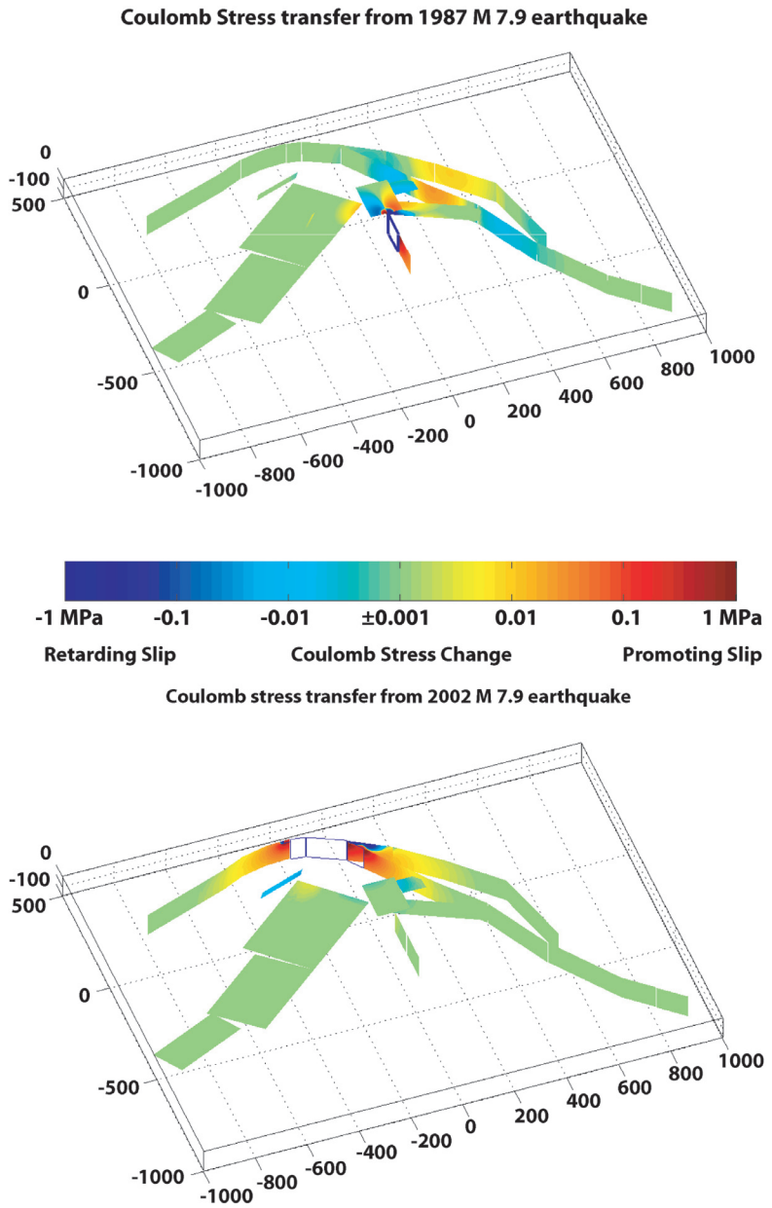

Plate 5. View looking N20°E and showing static Coulomb stress transferred from the rupture of (a, above the color bar) the *M* 7.9 Gulf of Alaska (north) earthquake of 1987. The downward-extended fault plane of the shallow strike-slip source is outlined in black. (b, below the color bar) The *M* 7.9 Denali fault earthquake of 2002. The downward-extended fault planes of the shallow strike-slip sources are outlined in black.

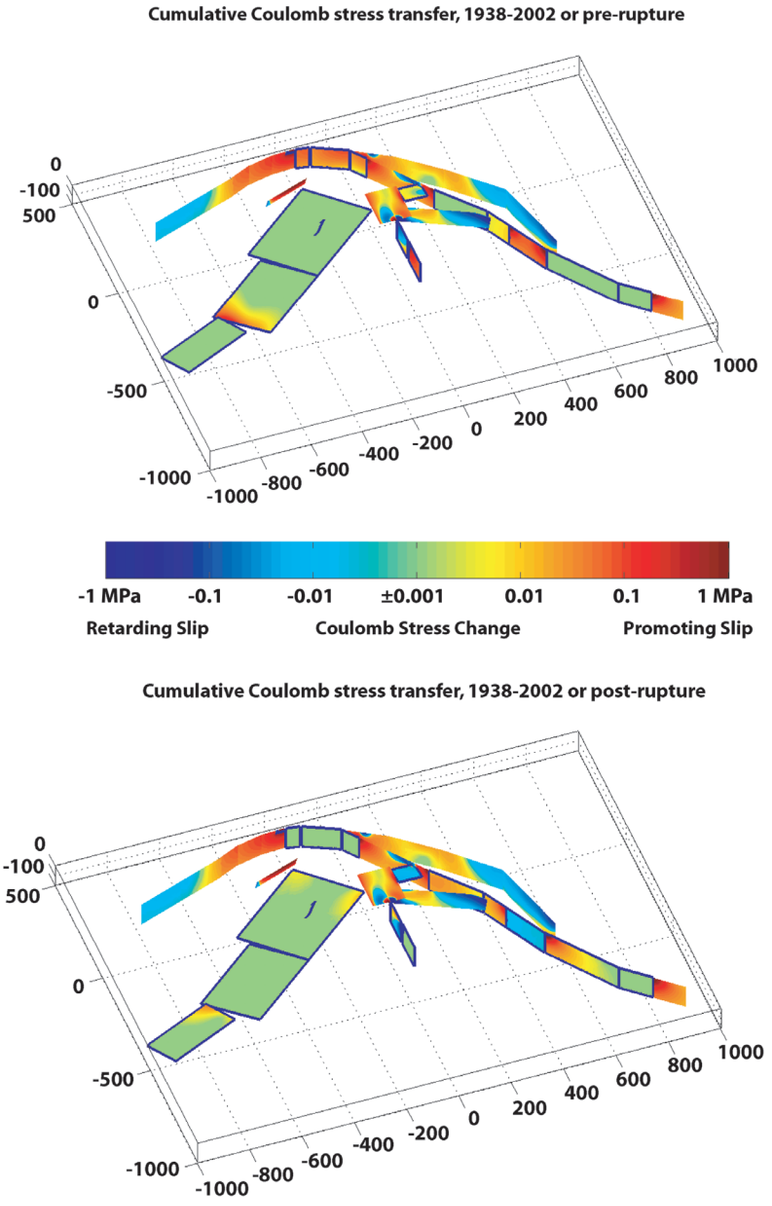

Plate 6. Views looking N20°E and showing cumulative static Coulomb stress transferred from the source ruptures (Table 1) to each of the target segments (Table 2). Shallow strike-slip source zones are extended downward for better visibility. (a, above the color bar) For target segments that are part of an (outlined) source rupture, cumulative stresses received before failure are shown. (b, below the color bar) For target segments that are part of an (outlined) source rupture, cumulative stresses transferred from sources that postdate the segment rupture are shown (current, December 2007).

transfer of strain from the shallow regions of rupture may result in slow postseismic viscoelastic deformation in the upper mantle [*Pollitz et al*., 1998] that slowly propagates to great distances. These questions are central to development of useful time-dependent earthquake probability models. Excellent overviews of the implications of Coulomb stress transfer for earthquake hazard have been provided by *Simpson* [2003], *Hardebeck* [2004], and *Parsons* [2005]. *Boyd et al*. [this volume] have used combined static (coseismic) and postseismic Coulomb stress transfer in a time-dependent earthquake probability model to generate time-dependent probabilistic earthquake hazard maps for Alaska.

8. CONCLUSIONS

1. As expected, stress transferred by the failure of adjacent segments dominates the cumulative coseismic Coulomb stress maps for eastern Alaska. An exception is the stress transferred over 150 km from the great Prince William Sound earthquake of 1964 to the north-central Denali fault.
2. Active fault segments are almost universally moved closer to failure by cumulative transferred stresses. Thus Coulomb stress transfer is helpful in identifying those faults that are likely to be currently most active. The cumulative stress shadow at seismogenic depths on a vertical strike-slip segment in the Totschunda–Fairweather gap may indicate that this connecting segment, which is largely covered by glaciers, does not exist. This gap may be a thrust regime [*Bird*, 1996; *Bufe*, 2004b]. There are no major stress shadows after the great 1964 Alaska earthquake, as seen after the 1906 San Francisco earthquake.
3. In addition to providing spatial information on earthquake hazard, static Coulomb stress transfer, in hindsight, identified those segments most likely to fail within a few decades. Stresses in excess of 0.1 MPa were transferred to several of the eastern Alaska segments during the 1938–2002 period. The posttransfer remaining times to failure for these segments ranged from 3 months to 38 years, indicating that these segments were nearing the end of their recurrence cycles and/or were triggered by large, time-dependent post-earthquake stress transfer processes.
4. Coulomb stress transferred to faults with lower slip rates, such as the Denali fault, has a greater impact. This has also been noted by *Hardebeck* [2004] and *Parsons* [2005].
5. While static Coulomb stress transfer is immediate, triggering of $M \geq 7.5$ events is not. There appears to be at least a 3-month waiting period, even for adjacent segments as in the case of the November 1987 and March 1988 high-stress events in the Gulf of Alaska.
6. Anelastic processes (creep, viscoelastic relaxation) probably result in concentration of transferred stress around large asperities, with triggering typically months to decades later [see also *Boyd et al*., this volume).

Acknowledgments. We thank Rob Wesson for his ongoing enthusiasm, guidance, and support. We also wish to express our gratitude to Yuehua Zeng, Jeanne Hardebeck, and Jeanne Sauber for their constructive reviews of the manuscript at various stages of its preparation, and to Goran Ekstrom for his editorial contributions.

REFERENCES

Anderson, G., and C. Ji (2003), Static stress transfer during the 2002 Nenana Mountain–Denali Fault, Alaska, earthquake sequence, *Geophys. Res. Lett.*, *30*, doi:10.1029/2002GL016724.

Bird, P. (1996), Computer simulations of Alaskan neotectonics, *Tectonics*, *15*, 225–236.

Boyd, O. S., F. F. Pollitz, Y. Zeng, J. L. Hardebeck, C. G. Bufe, R. L. Wesson, C. S. Mueller, A. Frankel, and M. D. Petersen (2007), Time-dependent probabilistic seismic hazard analysis for Alaska, this volume.

Bufe, C. G. (2004a), Comparing the November 2002 Denali and November 2001 Kunlun earthquakes, *Bull. Seismol. Soc. Am.*, *94*, 1159–1165.

Bufe, C. G. (2004b), Stress transfer to the Denali and other regional faults from the *M* 9.2 Alaska earthquake of 1964, *Bull. Seismol. Soc. Am*., *94*(6B), S145–S155.

Bufe, C. G. (2005), Stress distribution along the Fairweather–Queen Charlotte transform fault system, *Bull. Seismol. Soc. Am*., *95*(5), 2001–2008, doi:10.1785/0120040171.

Bufe, C. G. (2006), Coulomb stress transfer and tectonic loading preceding the 2002 Denali fault earthquake, *Bull. Seismol. Soc. Am*., *96*(5), 1662–1674, doi:10.1785/0120050007.

Bufe, C. G., and D. J. Varnes (1993), Predictive modeling of the seismic cycle of the greater San Francisco Bay region, *J. Geophys. Res.*, *98*, 9871–9883.

Bufe, C. G., S. P. Nishenko, and D. J. Varnes (1994), Seismicity trends and the potential for large earthquakes in the Alaska–Aleutian region, *Pure Appl. Geophys*., vol. 142, Special Issue on Shallow Subduction Zones, edited by R. Dmowska and G. Ekstrom, pp. 83–99.

Choy, G. L., and A. McGarr (2002), Strike-slip earthquakes in the oceanic lithosphere: Observations of exceptionally high apparent stress, *Geophys. J. Int.*, *150*, 506, 10.1046/j.1365-246X.2002.01720.x.

Dieterich, J. (1994), A constitutive law for rate of earthquake production and its application to earthquake clustering, *J. Geophys. Res*., *99*, 2601–2618.

Eberhart-Phillips, D. et al. (2003), The 2002 Denali fault earthquake, Alaska: A large magnitude, slip-partitioned event, *Science*, *300*, 1113–1118.

Estabrook, C. H., J. L. Nabelek, and A. L. Lerner-Lam (1992), Tectonic model of the Pacific–North American plate boundary in the Gulf of Alaska from broadband analysis of the 1979 St. Elias, Alaska, earthquake and its aftershocks, *J. Geophys. Res*., *97*, 6587–6612.

Fletcher, H. J., and J. T. Freymueller (2003), New constraints on the motion of the Fairweather fault, Alaska, from GPS observations, *Geophys. Res. Lett*., *30*, 10.1029/2002GL016476.

Frankel, A. (2004), Rupture process of the M7.9 Denali fault, Alaska, earthquake: Sub-events, directivity, and scaling of high-frequency ground motions, *Bull. Seismol. Soc. Am*., *94*(B), S234–S255.

Global CMT Catalog (2007), formerly Harvard CMT Catalog, maintained by Goran Ekstrom and Meredith Nettles. (Available at www.globalcmt.org).

Gomberg, J., and M. Ellis (1994), Topography and tectonics of the central New Madrid seismic zone: Results of numerical experiments using a three-dimensional boundary element program, *J. Geophys. Res*., *99*, 20,299–20,310.

Gomberg, J., P. Bodin, K. Larson, and H. Dragert (2004), Earthquake nucleation by transient deformations caused by the *M* = 7.9 Denali, Alaska, earthquake, *Nature*, *427*, 621–624.

Hardebeck, J. L. (2004), Stress triggering and earthquake probability estimates, *J. Geophys. Res., 109*, B04310, doi:10.1029/2003JB002437.

Hreinsdottir, S., J. T. Freymueller, H. J. Fletcher, C. F. Larsen, and R. Burgmann (2003), Coseismic slip distribution of the 2002 M_w7.9 Denali fault earthquake, Alaska, determined from GPS measurements, *Geophys. Res. Lett*., *30*, 1670, doi:10.1029/2003GL017447.

Hreinsdottir, S., J. T. Freymueller, R. Burgmann, and J. Mitchell (2006), Coseismic deformation of the 2002 Denali fault earthquake: Insights from GPS measurements, *J. Geophys. Res*., *111*, B03308, doi:10.1029/2005JB003676.

Johnson, J., Y. Tanioka, L. Ruff, K. Satake, H. Kanamori, and L. Sykes (1994), The 1957 great Aleutian earthquake, *Pure Appl. Geophys*., *142*, 3–28.

Johnson, J. M., and K. Satake (1994), Rupture extent of the 1938 Alaskan earthquake as inferred from tsunami waveforms, *Geophys. Res. Lett*., *21*, 733–736.

Johnson, J. M., K. Satake, S. R. Holdahl, and J. Sauber (1996), The 1964 Prince William Sound earthquake: Joint inversion of tsunami and geodetic data, *J. Geophys. Res*., *101*, 523–532.

Mazzotti, S., R. D. Hyndman, P. Fluck, and A. J. Smith (2003), Distribution of the Pacific/North America motion in the Queen Charlotte Islands–S. Alaska boundary zone, *Geophys. Res. Lett*., *30*, doi:10.1029/2003GL017586.

Nishenko, S. P., and K. H. Jacob (1990), Seismic potential of the Queen Charlotte–Alaska–Aleutian seismic zone, *J. Geophys. Res*., *95*, 2511–2532.

Okada, Y. (1992), Internal deformation due to shear and tensile faults in a half space, *Bull. Seismol. Soc. Am*., *82*, 1018–1040.

Pacheco, J. F., and L. R. Sykes (1992), Seismic moment catalog of large shallow earthquakes, 1900 to 1989, *Bull. Seismol. Soc. Am*., *82*, 1306–1349.

Page, R. A., N. N. Biswas, J. C. Lahr and H. Pulpan (1991), Seismicity of continental Alaska, in *Neotectonics of North America*, *Decade Map Volume 1*, edited by D. B. Slemmons, E. R. Engdahl, M. D. Zoback, and D. D. Blackwell, Geol. Soc. of Am., Boulder, Colo.

Parsons, T. (2005), Significance of stress transfer in time-dependent earthquake probability calculations, *J. Geophys. Res*., *110*, B05S02, doi:10.1029/2004JB003190.

Parsons, T., S. Toda, R. S. Stein, A. Barka, and J. H. Dieterich (2000), Heightened odds of large earthquakes near Istanbul: An interaction-based probability calculation, *Science*, *288*, 661–665.

Plafker, G., L. Gilpin, and J. Lahr (1994), Neotectonic map of Alaska, in *Geology of Alaska, Geology of North America, G-1*, Geol. Soc. of Am., Boulder, Colo.

Pollitz, F. F., R. Bürgmann, and B. Romanowicz (1998), Viscosity of oceanic asthenosphere inferred from remote triggering of earthquakes, *Science*, *280*, 1245–1249.

Rogers, G. C. (1986), Seismic gaps along the Queen Charlotte fault, *Earthquake Predict. Res., 4*, 1–11.

Sauber, J. M., T. A. Clark, L. J. Bell, M. Lisowski, C. Ma, and D. S. Caprette (1993), Geodetic measurement of static displacement associated with the 1987–1988 Gulf of Alaska earthquakes, in *Contributions of Space Geodesy to Geodynamics*, edited by D. E. Smith and D. L. Turcotte, pp. 233–248, AGU Geodynamics Series, Washington, D. C.

Schell, M. M., and L. J. Ruff (1989), Rupture of a seismic gap in southeastern Alaska: The 1972 Sitka earthquake (M_s 7.6), *Phys. Earth Planet. Inter.*, *54*, 241–257.

Simpson, R. W. (2003), Estimated changes in state on San Francisco Bay region faults resulting from the 1906 and 1989 earthquakes, in Working Group on California Earthquake Probabilities, Earthquake Probabilities in the San Francisco Bay Region: 2002–2031, *U. S. Geol. Surv. Open File Rep*., *03-214*, Appendix F, 30 pp.

Stephens, C. D., J. C Lahr, K. A. Fogleman, and R. B. Horner (1980), The St. Elias, Alaska, earthquake of February 28, 1979: Regional recording of aftershocks and short-term, pre-earthquake seismicity, *Bull. Seismol. Soc. Am*., *70*, 1607–1633.

Toda, S., R. S. Stein, K. Richards-Dinger, and S. Bozkurt (2005), Forecasting the evolution of seismicity in southern California: Animations built on earthquake stress transfer, *J. Geophys. Res*., *110*, B05S16, doi:10.1029/2004JB003415.

Wesson, R. L., A. D. Frankel, C. S. Mueller, and S. C. Harmsen (1999), Probabilistic seismic hazard maps of Alaska, *U.S. Geol. Surv. Open File Rep*., *99-36*, 43 pp.

C. G. Bufe, U.S. Geological Survey, Golden, CO 80401, USA.

O. S. Boyd, U.S. Geological Survey, Memphis, TN 38152-3050, USA. (geoling@gmail.com with a cc: to cbufe@usgs.gov)